AGU PUBLICATIONS

JGR

Journal of Geophysical Research: Atmospheres

RESEARCH ARTICLE
10.1002/2015JD023610

Key Points:
- The tree ring $\delta^{18}O$ is a promising proxy to reconstruct precipitation
- No juvenile effect on tree ring $\delta^{18}O$ is present for *P. taiwanensis*
- Most of extreme events that were identified by tree ring $\delta^{18}O$ are recorded in the documentaries

Correspondence to:
J. Ge,
gejunyi@ivpp.ac.cn

Citation:
Xu, C., J. Ge, T. Nakatsuka, L. Yi, H. Zheng, and M. Sano (2016), Potential utility of tree ring $\delta^{18}O$ series for reconstructing precipitation records from the lower reaches of the Yangtze River, southeast China, *J. Geophys. Res. Atmos.*, *121*, 3954–3968, doi:10.1002/2015JD023610.

Received 21 MAY 2015
Accepted 31 MAR 2016
Accepted article online 6 APR 2016
Published online 27 APR 2016

Potential utility of tree ring $\delta^{18}O$ series for reconstructing precipitation records from the lower reaches of the Yangtze River, southeast China

Chenxi Xu[1,2], Junyi Ge[3,4], Takeshi Nakatsuka[2], Liang Yi[5], Huaizhou Zheng[6,7], and Masaki Sano[2]

[1]Key Laboratory of Cenozoic Geology and Environment, Institute of Geology and Geophysics, Chinese Academy of Sciences, Beijing, China, [2]Research Institute for Humanity and Nature (RIHN), Kyoto, Japan, [3]Key Laboratory of Vertebrate Evolution and Human Origins of the Chinese Academy of Sciences, Institute of Vertebrate Paleontology and Paleoanthropology, Chinese Academy of Sciences, Beijing, China, [4]CAS Center for Excellence in Tibetan Plateau Earth Sciences, Beijing, China, [5]State Key Laboratory of Marine Geology, Tongji University, Shanghai, China, [6]Key Laboratory of Humid Subtropical Eco-Geographical Process, Ministry of Education, Fuzhou, China, [7]College of Geographical Sciences, Fujian Normal University, Fuzhou, China

Abstract In this study, we investigated the interannual and intraannual variabilities in the oxygen isotope composition ($\delta^{18}O$) preserved in the tree ring cellulose of *Pinus taiwanensis* in the lower reaches of the Yangtze River, southeast China, to explore its potential utility for precipitation reconstruction over the period of 1855–2013. Intraannual variations of tree ring cellulose $\delta^{18}O$ show distinct annual cycles that are characterized by $\delta^{18}O$ maxima in the early growth near the ring boundary and $\delta^{18}O$ minima in the middle and late portions of the ring. Seasonal patterns of tree ring $\delta^{18}O$ were influenced by August–October typhoons. The tree ring cellulose $\delta^{18}O$ was measured in both young and old trees to test for the juvenile effect. The results revealed no significant differences in the mean values and long-term trends in $\delta^{18}O$ in the old and young trees. A response analysis indicated that tree ring $\delta^{18}O$ correlated significantly with precipitation and relative humidity between May and October, and the $\delta^{18}O$ chronology accounted for 37.4% of the actual variation in the May–October precipitation between 1951 and 2013. The extremely dry and wet years revealed by the tree ring $\delta^{18}O$-based reconstructed precipitation also corresponded to actual local drought and flood events from the documentary records. Reconstructed precipitation showed significant relationship with central tropical Pacific sea surface temperature, which indicated that El Niño–Southern Oscillation (ENSO) exerted influences on May–October precipitation in the lower reaches of the Yangtze River. In addition, the relationship between ENSO and precipitation weakened between 1920 and 1940, and low variance of ENSO from 1920 to 1940 may result in the damped ENSO's influences on precipitation in southeast China.

1. Introduction

The Asian summer monsoon (ASM) significantly influences the agriculture and economy of monsoonal Asia. However, current climate models are unable to simulate ASM variations with complete accuracy; for example, the multimodel mean interannual rainfall anomalies for the El Niño–Southern Oscillation (ENSO) monsoon teleconnection are weaker than the observed values [*Sperber et al*., 2012]. Extensive time series of precipitation data are vital for the evaluation of climate variability and change, but most observational precipitation records obtained from Chinese weather stations only date back to 1951. Based on short precipitation records from meteorological stations, it is difficult to get ASM changes from multidecadal to centennial time scales, which are important to understand the mechanism of ASM and assess possible changes of ASM. The geological and biological records which are affected by monsoon season precipitation could provide precipitation information in multidecadal and centennial time scales.

Tree ring data are commonly used to reconstruct climate records because of its widespread distribution and accurate high-resolution dating [*Fritts*, 1976]. However, there have been few dendroclimatological studies in the subtropical regions of southeast China because old trees are scarce and cross dating is difficult. The lack of obvious factors controlling tree growth also makes it difficult to extract climate information from ring width. Nonclimatic disturbances usually have a major impact on the growth patterns of individual trees. Recently, winter temperatures were reconstructed using ring width data from the Taiwanese

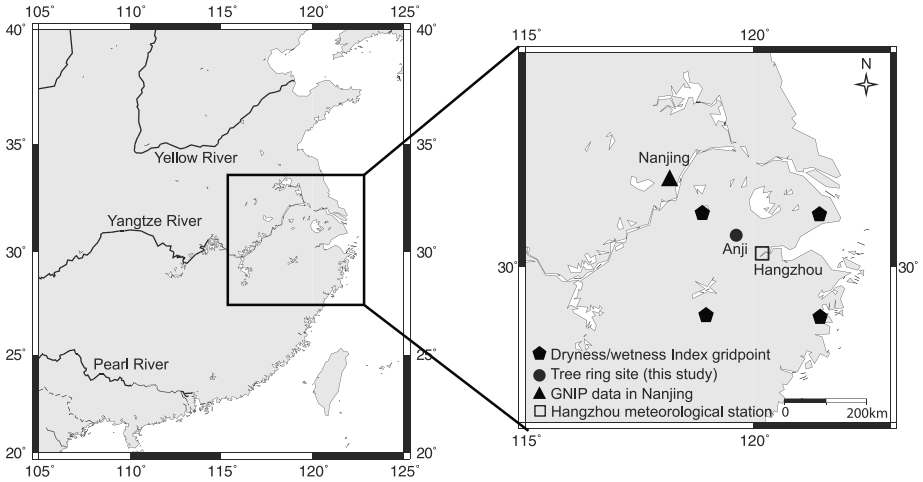

Figure 1. The study region and sampling location.

pine, *Pinus taiwanensis*, in southeast China [*Shi et al*., 2010; *Duan et al*., 2012]. In eastern China, historical documents can be used to reconstruct precipitation. For example, the "Clear and Rain Records" preserved in the Qing Dynasty Royal Archive contain daily weather reports and were used to reconstruct the seasonal and annual precipitation in Nanjing, Suzhou, and Hangzhou during the eighteenth century [*Zhang et al*., 2005]. However, such records that are helpful for climate reconstruction exist in only four cities. Similarly, the Yu-Xue-Fen-Cun (ancient rainfall and snowfall data) archives from the Qing Dynasty are robust proxies for the amounts of precipitation on different time scales [*Ge et al*., 2005; *Wu et al*., 2010] but are only available for the period of 1736–1911 [*Ge et al*., 2005]. The dryness–wetness index (DWI) [*Zhang*, 1988] contained in Chinese historical documents from eastern China also reflects the precipitation variations in summer, but the DWI is only semiquantitative and noncontinuous at many sites [*Song*, 2000; *Qian et al*., 2006].

Tree ring oxygen isotopes show a more robust and stronger climatic signal than ring width for trees in tropical areas [*Xu et al*., 2011]. Climate information can typically be extracted from tree ring isotope series even in situations where the ring width chronology shows no significant correlation with climate parameters [*Xu et al*., 2011, 2013a]. *Feng et al*. [1999] showed that tree ring hydrogen isotopes can be used as an indicator of Asian monsoon intensity, but hydrogen isotope series obtained from *Cryptomeria fortune* in Tianmushan, southeast China, correlated positively with the October–November minimum temperature [*Qian et al*., 2002a]. However, tree ring carbon isotopes from *Cryptomeria fortune* in Tianmushan are correlated positively with January, March, and June–July precipitation [*Qian et al*., 2002b] but showed a close relationship with September precipitation and September–December temperatures [*Zhao et al*., 2005]. This inconsistent climate sensitivity shown by tree ring carbon isotopes is not useful for reconstructing historical precipitation records.

Tree ring cellulose oxygen isotopes are mainly controlled by the isotopic composition of the source water and the relative humidity [*Roden et al*., 2000]. The isotopic composition of the source water generally follows that of the oxygen isotopes in precipitation, which correlates negatively with the amount of rainfall during the rainy season (i.e., the "amount effect") [*Dansgaard*, 1964; *Liu et al*., 2010]. Relative humidity also correlates positively with rainfall. Therefore, tree ring oxygen isotope series can potentially record the amount of rainfall in areas where the amount effect occurs. Previous studies have shown that tree ring oxygen isotopes reflect regional rainy season precipitation in Laos [*Xu et al*., 2013a], Thailand [*Xu et al*., 2015], Bhutan [*Sano et al*., 2013], and Fujian, a subtropical region of southeast China [*Xu et al*., 2013b]. In this study, we analyzed the tree ring cellulose oxygen isotopes preserved in young and old *P. taiwanensis* from the lower reaches of the Yangtze River in southeast China over the period of 1850–2013, at both annual and seasonal resolution, and explore the potential utility of tree ring cellulose $\delta^{18}O$ in reconstructing precipitation records.

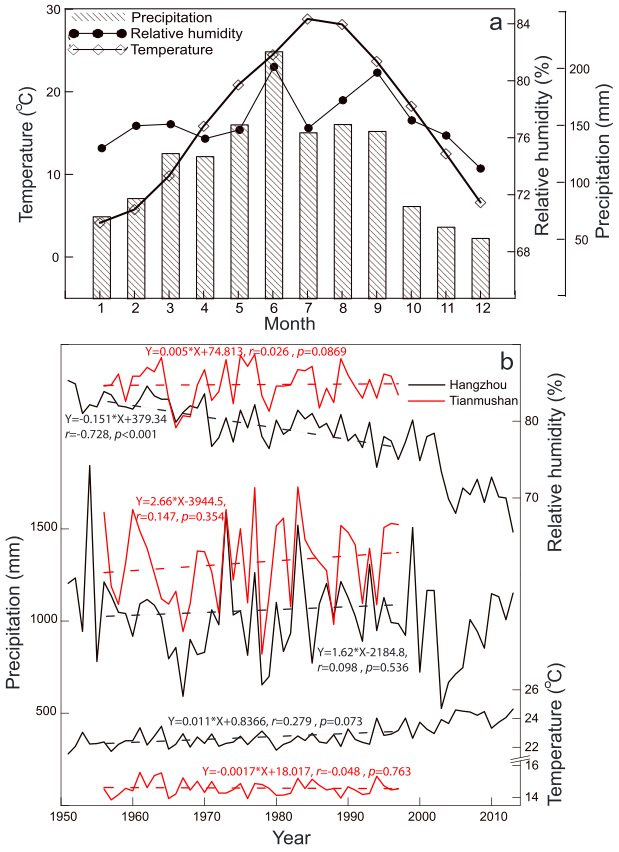

Figure 2. (a) Monthly climate in Hangzhou. (b) Interannual variations and long-term trend of total precipitation, mean temperature, and relative humidity from April to October at the Hangzhou (black line) and Tianmushan (red line) meteorological station.

2. Materials and Methods

2.1. Sampling Sites and Cross Dating

Tree ring samples were collected using increment borers (5 mm diameter) at breast height from *P. taiwanensis* forests near Anji (AJ) County (30.39°N, 119.43°E; 1482 m above sea level (asl)), which is located 70 km west of Hangzhou City, southeast China (Figure 1). *P. taiwanensis* grows at moderate to high altitudes on steep, rocky crags and is the dominant tree species in the forest. The growth season is from April to October [*He et al.*, 2012]. *P. taiwanensis* has a shallow root system, which is characterized by well-developed horizontal roots, and more than 80% of large roots and 75% of fine roots are distributed between the surface and a depth of 30 cm [*Yen*, 1972]. The maximum depth of root development is less than 60 cm [*Yen*, 1972]. Therefore, tree ring cellulose $\delta^{18}O$ is expected to record the $\delta^{18}O$ of the precipitation and relative humidity during the growth season.

Cores were collected from 71 trees. The cores were air dried and polished until the ring structure was clearly visible. The ring widths were measured at a resolution of 0.01 mm using a sliding stage micrometer linked to a computer (Velmex™, ACU-RITE). Cross dating was performed by matching variations in the ring widths in all cores, and the COFECHA software [*Holmes*, 1983] was used for quality control.

2.2. Meteorological Data

Hangzhou meteorological station (30.23°N, 120.17°E; 42 m asl) is located about 70 km from the sampling site. The mean annual precipitation was 1423 mm during the period of 1951–2014. The highest monthly precipitation occurred in June, and the main rainy season was from May to September (Figure 2a). The mean annual relative humidity was 77.4%, and the monthly relative humidity reached its peak in June (81.3%). However, Hangzhou is a big city which may be affected by the urbanization; we compared meteorological data from Tianmushan (30.35°N, 119.42°E; 1506 m asl) and Hangzhou during the common period of 1957–1997. Tianmushan station is located about 25 km from the sampling site in rural area. Interannual variations in the mean temperature, total precipitation, and relative humidity during the growth season for both meteorological stations are illustrated in Figure 2b. Interannual variations of relative humidity, precipitation, and temperature from Hangzhou and Tianmushan station are similar, but long-term trends of relative humidity and temperature are different (Figure 2b). Relative humidity in Hangzhou shows a significant decreasing trend, while there is no significant trend for relative humidity in Tianmushan, which may reflect the influences of urbanization in Hangzhou. However, precipitation in Hangzhou and Tianmushan do not show any significant trend during the period of 1956–1997. Although climate data from Tianmushan station may not be affected by urbanization, it is not available after 1998. Climate data from Hangzhou covering the period of 1951–2014 were used for climate response analysis, and we removed the significant trend for relative humidity and temperature before correlation analysis.

2.3. Stable Isotopic Analysis

Four cores from the young trees (AJ2, AJ303, AJ312, and AJ320) and from the old trees (AJ12, AJ17, AJ29, and AJ21) were selected for isotopic analysis to test potential juvenile effect. The average ages of the young and old trees were about 70 and 150 years, respectively. Most of the cores reached the pith of the tree. The rings (1983–1993) that were relatively wide in core AJ8 were selected for intraannual isotope analysis. Each ring is divided into six samples by hand with a razor knife. The modified plate method [*Xu et al*., 2011, 2013a], which extracts the α-cellulose directly from the wood plate rather than from individual rings, was used to reduce the time required for the procedure.

We loaded the cellulose samples (sample weight, 80–260 μg) into silver foil and measured the $^{18}O/^{16}O$ ratios using an isotope ratio mass spectrometer (Delta V ADVANTAGE, Thermo Scientific, USA) interfaced with pyrolysis-type elemental analyzer (TC/EA) at the Research Institute for Humanity and Nature, Japan. The isotopic results for oxygen are presented in δ notation as per mil (‰) relative to the Vienna standard mean ocean water: $\delta^{18}O = [(R_{sample}/R_{standard}) - 1] \times 1000‰$, where R_{sample} and $R_{standard}$ are the $^{18}O/^{16}O$ ratios of the sample and standard, respectively. The cellulose $\delta^{18}O$ values were calculated by comparison with the laboratory working standard (Merck cellulose, 27.4‰), which was inserted every eight samples during the measurement runs. The analytical uncertainties associated with the repeated measurements of the Merck cellulose and cellulose sample were 0.13‰ ($n = 113$) and ±0.3‰ ($n = 10$), respectively.

2.4. Climatic and Statistical Analyses

The gridded precipitation data sets from the Global Precipitation Climatology Centre (GPCC) Full Reanalysis version 7 (v7) analysis (119–120°E, 30–31°N; ftp://ftp.dwd.de/pub/data/gpcc/html/), with a resolution of 0.5° × 0.5°, were used to evaluate the climatic sensitivity of the tree ring cellulose $\delta^{18}O$ series. The Royal Netherlands Meteorological Institute Climate Explorer (http://www.knmi.nl/) was also used to examine the spatial correlation between the oxygen isotope chronology and the sea surface temperature (SST) from the National Climatic Data Center v3b data set [*Smith et al*., 2008]. Gridded points for DWI near the study area [*Zhang*, 1988; *Yang et al*., 2013], which were derived from historical documents from eastern China, were used to test the reliability of the reconstructed May–October precipitation. DWI has five grades: very wet (grade 1), wet (grade 2), normal (grade 3), dry (grade 4), and very dry (grade 5). The precipitation $\delta^{18}O$ data from Nanjing (1987–1992; 32°03′N, 118°46′E; International Atomic Energy Agency database: www.iaea.org) were used to evaluate the seasonal variations in tree ring $\delta^{18}O$.

To test the typhoon's influence on seasonal pattern of tree ring $\delta^{18}O$, typhoon activity history from documentary is used [*Wen*, 2006]. Based on August–October typhoons' landing positions and influences on sampling site, 1983, 1986, 1991, and 1993 are selected as nontyphoon years, while 1984, 1985, 1987–1990, and 1992 are identified as typhoon years [*Wen*, 2006] during the period of 1983–1993. The expressed population signal (EPS) is higher than 0.85, which indicates that the composite record accurately represents the mean variance of the population. $EPS = (n \times r_{mean})/[(n \times r_{mean}) + (1 - r_{mean})]$, where r_{mean} is the mean correlation coefficient among all samples and n is the number of trees that are measured at the study site. To evaluate the validity of the linear regression model between tree ring $\delta^{18}O$ and precipitation, two subperiods (1951–1982 and 1983–2013) were split for separate calibration and verification. The Pearson's correlation coefficient (r), explained variance (r^2), reduction of error (RE), and coefficient of efficiency (CE) were included in calibration and verification statistical tests [*Cook et al*., 1999]. Superposed epoch analysis (SEA) was used to examine relationship between extreme events which are identified by tree ring $\delta^{18}O$ and extreme events from historical documentaries.

3. Results and Discussion

3.1. Intraannual Variability of Tree Ring $\delta^{18}O$

The variations in the intraannual tree ring $\delta^{18}O$ values, which are associated with the climate during the growth season [*Evans and Schrag*, 2004; *Managave et al*., 2010; *Xu et al*., 2014, 2016], can provide climate information at a high resolution (monthly, even weekly) and improve our understanding of the climatic implications of annual tree ring $\delta^{18}O$. The intraannual $\delta^{18}O$ values for *P. taiwanensis* show well-defined annual cycles, which are characterized by $\delta^{18}O$ maxima in the early growth near the ring boundary and $\delta^{18}O$ minima in the middle and late portions of the ring (Figure 3a). The range of the seasonal $\delta^{18}O$ variations was around

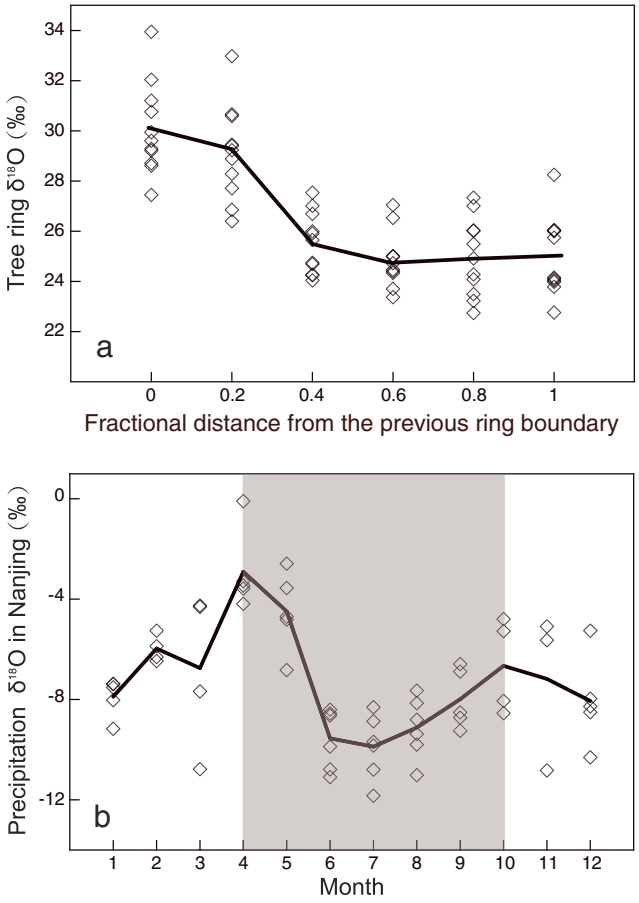

Figure 3. (a) Intraannual variations in tree ring cellulose $\delta^{18}O$. (b) Monthly precipitation $\delta^{18}O$ in Nanjing between 1987 and 1992.

6‰. The seasonality of the tree ring cellulose $\delta^{18}O$ generally followed the seasonal pattern of precipitation $\delta^{18}O$ in Nanjing (Figure 3b). Based on the monthly (Global Network for Isotopes in Precipitation) and daily [*Tang et al.*, 2015] precipitation $\delta^{18}O$ in Nanjing, precipitation $\delta^{18}O$ showed the most depleted values in summer due to strong convection and long-distance vapor transport and enriched values in September because of the ASM retreat and transportation of water vapor from inland area with enriched $\delta^{18}O$ [*Tang et al.*, 2015]. However, seasonal patterns of tree ring $\delta^{18}O$ did not show the enriched values in the late portion of the whole ring (Figure 3a). We investigated the seasonal pattern of tree ring $\delta^{18}O$ for each ring and found that enriched $\delta^{18}O$ in the late portion of the whole ring happened in the years when the study area was not influenced by typhoon in late growing season, while nonenriched $\delta^{18}O$ in the late portion of the whole ring appeared in the years when sampling site was affected by typhoon (Figure 4). Cellulose $\delta^{18}O$ values in the late portions of ring in typhoon years are lower than values obtained in nontyphoon years (Figure 4), and the differences between typhoon years and nontyphoon years for subannual part 5 and part 6 are ~0.8‰ and ~2.4‰, respectively. Because $\delta^{18}O$ of the precipitation and water vapor which are brought by typhoon are depleted [*Fudeyasu et al.*, 2008], ^{18}O-depleted precipitation in autumn brought by typhoons was absorbed by tree and ^{18}O-depleted signal was finally transferred to cellulose. Tree ring latewood $\delta^{18}O$ of longleaf pine in southeast United States has the potential to reconstruct tropical cyclone activity [*Miller et al.*, 2005], and seasonal pattern of tree ring $\delta^{18}O$ is useful to identify paleo-typhoon activity in the study area. However, to improve the understanding of the processes that typhoons affect seasonal pattern of tree ring $\delta^{18}O$, higher sampling resolution (e.g., 20 subsamples per ring) and more sampling sites from coastal zone to inland are needed in future study.

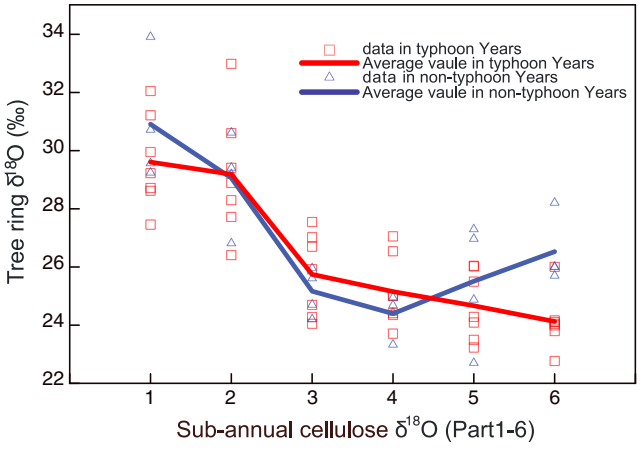

Figure 4. Intraannual cellulose $\delta^{18}O$ variations during typhoon years and nontyphoon years.

3.2. Signal Strength of Annual Tree Ring $\delta^{18}O$ Data

The cellulose $\delta^{18}O$ series from the old and young trees are shown in Figure 5. There are some missing data in the tree ring $\delta^{18}O$ time series (Figure 5), which

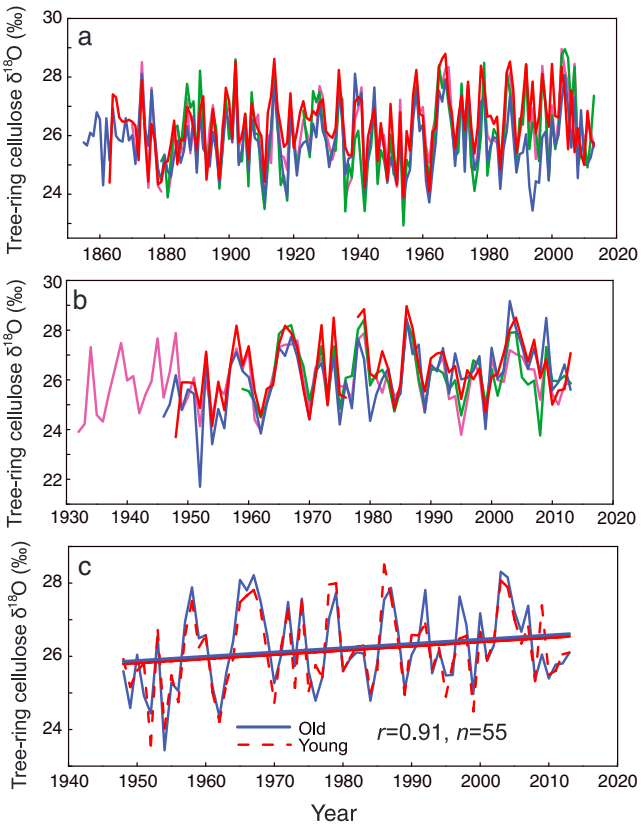

Figure 5. Annual tree ring cellulose $\delta^{18}O$ for (a) old and (b) young trees and (c) the $\delta^{18}O$ chronologies of the young and old trees over the common period (1948–2013).

can mostly be related to either the loss of several rings during the chemical treatment or the loss of cellulose samples during the oxygen isotopic measurement. The yearly $\delta^{18}O$ standard deviations for the four young and four old trees vary between 0.1‰ and 2.1‰ (mean = 0.5‰) and 0.2‰ and 1.9‰ (mean = 0.6‰), respectively. Table 1 presents the correlation coefficients (r) for the oxygen isotope time series used in the isotope analysis. The mean correlation coefficient for both young and old cores was 0.77. The EPS value for the $\delta^{18}O$ chronology for both old and young trees was 0.93, which is higher than the 0.85 [*Wigley et al.*, 1984]. The $\delta^{18}O$ chronologies for the old and young trees were produced by averaging four cores from each group. The mean values (standard deviations) for the $\delta^{18}O$ chronologies of the young and old trees during the common period of 1948–2013 were 26.17‰ (1.07‰) and 26.24‰ (1.11‰), respectively. The autocorrelations (1 year lag) of the $\delta^{18}O$ chronologies for the old and young trees were 0.21 and 0.19, respectively. The correlations between subannual parts of cellulose $\delta^{18}O$ and annual $\delta^{18}O$ are shown in Table 2, which reveal that from subannual part 1 to part 4 of cellulose $\delta^{18}O$ contribute the main variations for annual $\delta^{18}O$.

3.3. Juvenile Effect on Tree Ring $\delta^{18}O$

Cellulose $\delta^{18}O$ values of young oak trees in France increase by 2‰ in the first 30 years of growth [*Labuhn et al.*, 2013], but tree ring $\delta^{18}O$ for *Pinus uncinata* in Spain changes by –0.089‰ per decade over the first 100 years of growth [*Esper et al.*, 2010]. In contrast, *Sano et al.* [2013] reported that there was no apparent age-dependent bias for larch in Bhutan. Most tree ring chronologies (*Pinus massoniana* and *P. taiwanensis*) from southern China extend over less than 200 years [*Duan et al.*, 2013]. If we want to extract as much climate-related information from these chronologies as possible, an understanding of the juvenile effect on tree ring $\delta^{18}O$ in *P. taiwanensis* is needed.

Table 1. Correlations of Tree Ring $\delta^{18}O$ Between Old Trees

r	AJ17	AJ21	AJ20
AJ12	0.686[a]	0.715[a]	0.795[a]
AJ17		0.762[a]	0.796[a]
AJ21			0.863[a]
Correlations of tree ring $\delta^{18}O$ between young trees			
r	AJ303	AJ312	AJ320
AJ2	0.745[a]	0.816[a]	0.737[a]
AJ303		0.734[a]	0.743[a]
AJ312			0.844[a]

[a] $p < 0.01$.

The chronology obtained by averaging the four cores from the old and young trees showed similar interannual variations ($r = 0.91$, $n = 55$, $p < 0.0001$) during the common period of 1948–2013, and both the young and old trees showed increasing trends. These increasing trends in tree ring cellulose $\delta^{18}O$ over the last 50 years have also been reported in northern China [*Q. Li et al.*, 2011], northern Laos [*Xu et al.*, 2011], northern Vietnam [*Sano et al.*, 2012], Nepal [*Sano et al.*, 2011], and southwest

Table 2. Correlations Between Annual Tree Ring $\delta^{18}O$ and Subannual Tree Ring $\delta^{18}O$

r	Part 1	Part 2	Part 3	Part 4	Part 5	Part 6
Annual $\delta^{18}O$ versus subannual $\delta^{18}O$	0.743[a]	0.829[a]	0.620[a]	0.619[a]	0.505	0.499

[a] $p < 0.05$.

China [*Xu et al.*, 2012] and can be interpreted as the impact of the weakening ASM. The reduced intensity of the ASM may also increase the precipitation $\delta^{18}O$ and tree ring cellulose $\delta^{18}O$ [*Vuille et al.*, 2005; *Xu et al.*, 2011]. Therefore, the increasing trends in tree ring cellulose $\delta^{18}O$ in both the young and old trees sampled here reflect the effects of large-scale atmospheric circulation rather than age-related factors. Furthermore, there were no significant differences in the mean values or long-term trends in $\delta^{18}O$ between the old and young trees (Figure 5c). Therefore, no juvenile effect on $\delta^{18}O$ is present for *P. taiwanensis* that grow in the study area.

3.4. Climate Response

The correlations between the $\delta^{18}O$ chronologies obtained for the young and old trees and climatic parameters in Hangzhou station are shown in Figure 6. The tree ring cellulose $\delta^{18}O$ series for both the young

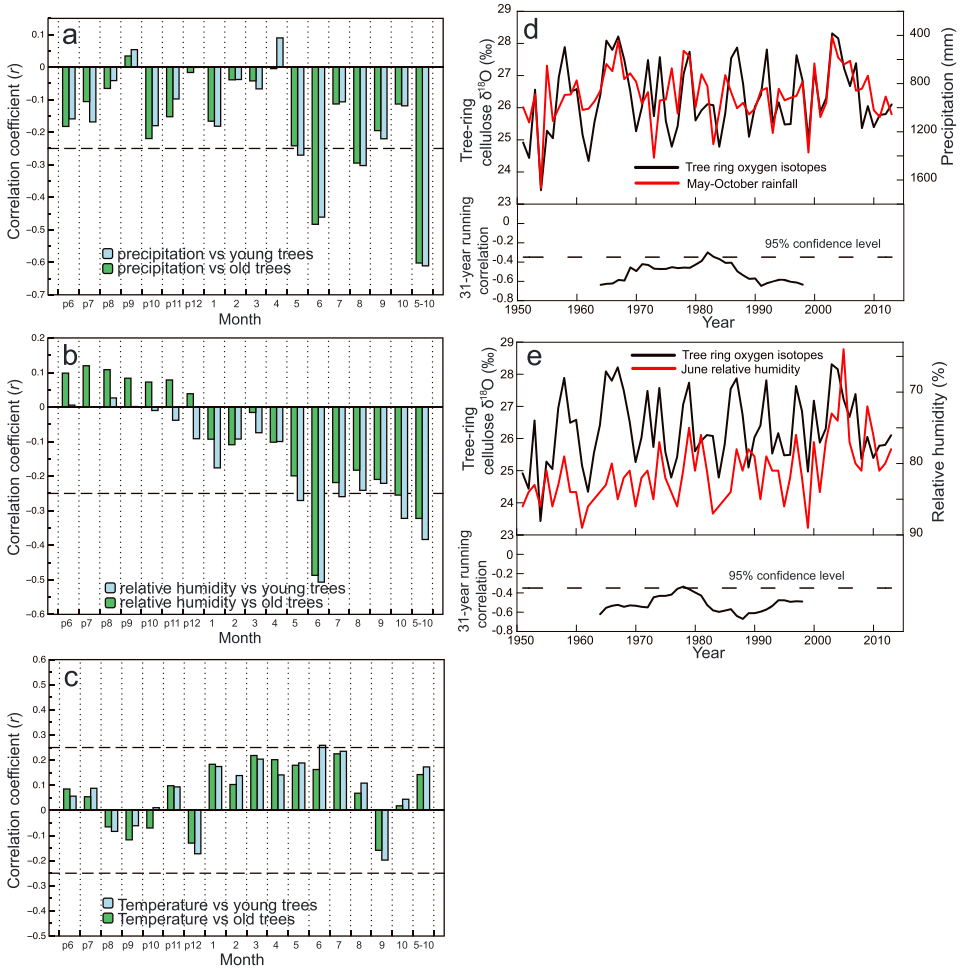

Figure 6. Correlations between (a) precipitation, (b) relative humidity, (c) temperature in Hangzhou station, and tree ring cellulose $\delta^{18}O$ from young and old trees; 31 year running correlations between (a) May–October precipitation/(e) June relative humidity and tree ring cellulose $\delta^{18}O$ from old trees.

Table 3. Calibration and Verification Statistics for the Period of 1951–2013

Calibration Period	R^2	Verification Period	r	RE	CE
Full (1951–2013)	0.374[b]	-	-	-	-
Early half (1951–1982)	0.390[b]	Late half (1983–2013)	0.612[b]	0.332[a]	0.326[a]
Late half (1983–2013)	0.375[b]	Early half (1951–1982)	0.624[b]	0.356[a]	0.352[a]

[a]RE, CE > 0.
[b]$p < 0.01$.

and old trees correlated significantly negatively with precipitation and relative humidity from May to October during the period of 1951–2013 (Figures 6a and 6b). The correlations between the regional precipitation data from GPCC v7 or the Climatic Research Unit Time series 3.21 and tree ring cellulose $\delta^{18}O$ showed similar results (not shown). Such negative correlations between precipitation in the growth season and tree ring cellulose $\delta^{18}O$ have also been observed at other sites in monsoonal Asia [*Sano et al*., 2012, 2013; *Xu et al*., 2013b, 2015]. The tree ring cellulose $\delta^{18}O$ series for both the young and old trees do not show significant correlations with temperature (Figure 6c).

Based on the tree ring cellulose isotope fractionation model [*Roden et al*., 2000], negative correlations are expected between tree ring cellulose $\delta^{18}O$ and relative humidity. Low relative humidity usually enhances evapotranspiration, which enriches leaf water $\delta^{18}O$ and also leads to the evaporation of soil water in the upper layer, so the source water $\delta^{18}O$ becomes heavier. Both these processes will lead to enriched tree ring cellulose $\delta^{18}O$.

Precipitation influences tree ring cellulose $\delta^{18}O$ mainly via relative humidity and precipitation $\delta^{18}O$. Precipitation usually has a positive relationship with relative humidity in the rainy season [*Xu et al*., 2013b]. For example, the correlation coefficient between relative humidity and precipitation at Hangzhou in June (highest monthly rainfall of the year) was 0.6. The negative relationship between the amount of precipitation and the precipitation $\delta^{18}O$ is known as the amount effect [*Dansgaard*, 1964] and has been demonstrated in observational data from southern China (Guangzhou; $r = -0.64$, $p < 0.001$) [*Liu et al*., 2010; *Xie et al*., 2011] and Southeast Asia [*Araguas-Araguas et al*., 1998], as well as in modeled data from southern China [*Yoshimura et al*., 2008]. The amount effect is caused by the depletion of air by condensation [*Vuille et al*., 2003]. Because the masses of $H_2{}^{18}O$ and $H_2{}^{16}O$ differ, isotope-enriched water vapor is more easily removed during the condensation process, which causes the isotopic composition of the remaining vapor to become lighter. Typically, the greater the amount of precipitation, the more depleted is the isotopic composition of this rainwater [*Vuille et al*., 2003]. Therefore, greater precipitation, which is associated with higher relative humidity and more $\delta^{18}O$-depleted precipitation, can lead to lower tree ring cellulose $\delta^{18}O$ (Figure 6a). Precipitation in June showed the highest correlation with the annual cellulose $\delta^{18}O$ ($r = -0.48$, $p < 0.001$), because the rainfall in June (Figure 2a) is high, and time-delayed nature of oxygen isotope signal transfers rainfall water to leaf water to cellulose. Water at the trunk base takes 2.5 to 21 days to reach the crown in coniferous species, and residence times ranged from 36 to 79 days [*Meinzer et al*., 2006]. The $\delta^{18}O$ signal was transferred from the leaf water to the cellulose with time lags of about 2 weeks [*Gessler et al*., 2009]. These caused the cellulose that formed in July and August to possibly contain the June rainfall signal. Furthermore, the $\delta^{18}O$ in both the young and old trees sampled here correlated similarly with precipitation and relative humidity.

Previous study [*Kanner et al*., 2013] revealed that tree ring $\delta^{18}O$ in Southern California has unstable correlations with soil water $\delta^{18}O$ and relative humidity. The climate shift happened in late 1970s in China [*Zhou et al*., 2009; *Huang et al*., 2015]. So 31 year running correlation analysis is utilized to evaluate the temporal correlation during the period of 1951–2013 between tree ring $\delta^{18}O$ and precipitation/relative humidity (Figures 5d and 5e). The stable correlations between tree ring $\delta^{18}O$ and May–October precipitation indicates the potential utility of tree ring $\delta^{18}O$ for precipitation reconstruction (Figure 5d).

3.5. Precipitation Reconstruction

May–October precipitation is considered to be the strongest predictor of variance in tree ring cellulose $\delta^{18}O$ ($r = -0.612$, $p < 0.001$) in the study area (Figure 6a). Therefore, tree ring $\delta^{18}O$ was used to reconstruct the

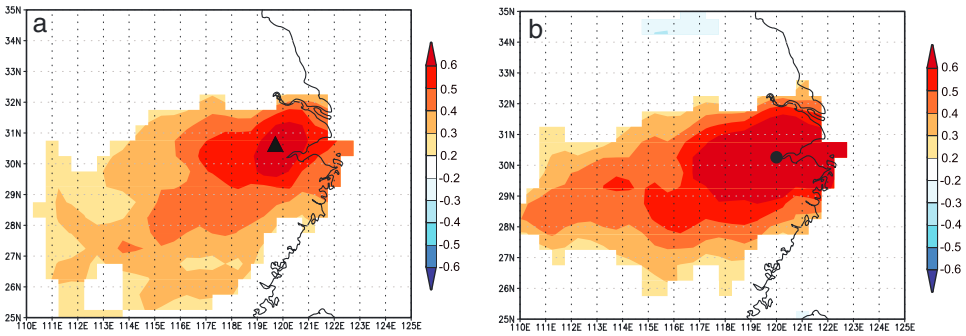

Figure 7. Spatial correlations between (a) tree ring cellulose δ^{18}O-based May–October precipitation reconstruction/(b) observed May–October precipitation and May–October precipitation from GPCC v7 over the periods of 1901–2013 and 1951–2013. The triangle indicates the sampling site, and the dot indicates the Hangzhou meteorological station.

May–October precipitation based on the transfer function between precipitation and tree ring δ^{18}O. The linear regression model explained 37.4% of the actual variance in the May–October precipitation. The reduction of error (RE) and coefficient of efficiency (CE; Table 3), which are the two most rigorous tests [*Cook et al.*, 1999], were both positive. These tests confirm the validity of the linear regression model derived here. In addition, tree ring δ^{18}O-based May–October precipitation reconstruction shows significant positive correlations with May–October precipitation in the Zhejiang and Jiangsu Provinces (Figure 7a) during the period of 1901–2013, and observational precipitation in Hangzhou shows similar results (Figure 7b).

Table 4. Extremely Wet Years Detected by the Tree Ring δ^{18}O-Based May–October Precipitation Reconstruction With Extremely Wet Events From Documentaries and Classified La Niña Events From *Gergis and Fowler* [2009]

Extremely Wet Years	Reconstructed May–October Precipitation (mm)	Flood Events in Documentaries	La Niña Year[b]
1875	1082.25	Flood in May and August at Lin'an[a]	S, S (1874)
1878	1115.94	Persistent rain at Gui'an	W
1879	1112.24	NA[c]	W (1878)
1881	1123.43	NA	VS (1880)
1882	1047.62	Flood in July at Lin'an, Deqing	NA
1893	1057.12	A great deal of rainfall in summer and autumn at Yuqian	VS, S (1892)
1897	1130.23	NA	W (1896)
1906	1090.08	Flood in August at Deqing	NA
1910	1048.85	Persistent rain from May to August at Deqing, a reduction in the grain yield	VS
1911	1174.15	Flood in Autumn at Lin'an, a reduction in the grain yield	VS (1910)
1917	1056.00	Flood in May at Jiaxing	VS, S (1916)
1918	1106.41	NA	S, VS (1917)
1936	1128.92	Persistent rain at Changhua resulted in flash floods and huge economic losses	NA
1937	1057.49	Flood in June at Zhejiang Province	NA
1938	1061.48	Flood in June at Changhua	NA
1942	1168.52	Persistent rain in summer at Fenshui	NA
1946	1059.94	Flood in late June at Lin'an, Hangzhou, Deqing	S, W (1945)
1949	1104.26	Persistent rain in June at Hang County; 20% of rice fields were flooded in Hang County	NA
1951	1063.65	Flood in July at Huzhou, Jiaxing	M, E (1950)
1952	1122.99	Flood in August and September in Huzhou	M (1951)
1954	1247.26	Longer Meiyu season (from May to July) at Zhejing Province; rainfall was 1.9 times than normal year	E (1953)
1962	1134.54	NA	W
1976	1079.49	NA	S (1975)
1984	1079.71	Flood in June at Hangzhou, Huzhou	M
1999	1056.66	Longer Meiyu season, rainstorm and flood in June at Hongzhou, Huzhou	E (1998)

[a]Sites that appear in the above table are located at Zhejiang Province.
[b]E: extreme; VS: very strong; S: strong; M: moderate; W: weak from *Gergis and Fowler* [2009].
[c]NA means not available.

Table 5. Extremely Dry Years Detected by the Tree Ring $\delta^{18}O$-Based May–October Precipitation Reconstruction With Extremely Dry Events From Documentaries and Classified El Niño Events From *Gergis and Fowler* [2009]

Extremely Dry Years	Reconstructed May–October Precipitation (mm)	Extremely Dry Events in Documentaries	El Niño Year[b]
1873	661.10	Severe droughts in summer and autumn at Deqing[a] and Gui'an caused a reduction in the grain yield	NA
1876	781.89	Drought in summer at Hangzhou	W
1891	775.80	NA[c]	VS
1899	787.47	Drought at Hangzhou	S
1902	627.82	A severe drought in the summer at Changhua	VS, S (1901)
1914	667.26	Drought in summer at Lin'an, Fenshui, Hangzhou	VS, VS (1913)
1928	762.60	NA	NA
1934	723.30	No rain from 5 August to 22 September	W (1933)
1945	780.20	Drought at Chunan	S (1944)
1958	696.06	Drought from June to late August in Hangzhou	M, S (1957)
1965	670.94	NA	S, S (1964)
1966	706.29	Drought from mid-July to October in western and northern Zhejiang Province	M, S (1965)
1967	654.97	Drought from June to October at Zhejiang Province	W, M (1966)
1968	743.80	NA	S, W (1967)
1972	746.00	NA	M
1974	734.53	NA	W (1973)
1979	714.19	NA	M
1986	738.07	Drought in July and August at Changhua	W (1985)
1987	697.80	NA	VS
1992	705.20	Drought from mid-July to early August at Zhejiang Province	VS, VS (1991)
1997	727.11	Drought from January to June at Hangzhou, Huzhou	W
2000	783.69	Drought at Anji County	NA
2003	643.20	Drought in July and August at Hangzhou	E (2002)
2004	662.06	NA	NA*[d]
2005	778.28	NA	NA*
2007	758.10	NA	NA*

[a]Sites that appear in the above table are located at Zhejiang Province.
[b]E: extreme; VS: very strong; S: strong; M: moderate; W: weak from *Gergis and Fowler* [2009].
[c]NA: not available.
[d]NA*: The El Niño event history from *Gergis and Fowler* [2009] ended in 2002, so there is no recorded El Niño event from *Gergis and Fowler* [2009] after 2003.

The mean value and standard deviation (SD) of the reconstructed May–October precipitation for 1855–2013 were 917 mm and 129 mm, respectively. Extremely wet years were defined with a value above one SD and an extremely dry year with a value below one SD. Based on this criteria, 26 extremely dry years and 25 extremely wet years were identified (Tables 4 and 5). The main wet periods from precipitation reconstruction were identified as 1875–1882 and 1936–1954.

To assess the accuracy of the reconstructed May–October precipitation, we compared it with the regional precipitation from GPCC v7 and the regional DWI (Figure 8). The correlation coefficient for the reconstructed precipitation and the regional precipitation from GPCC v7 was 0.48 ($p < 0.01$; 1901–2013). However, the relationship was not stable, and the correlation coefficient ($r = 0.68$, $p < 0.001$) for the period of 1951–2013 was higher than that for 1901–1950 ($r = 0.12$, $p = 0.26$). This low correlation between the reconstructed precipitation and the precipitation from GPCC v7 before 1951 has also been observed in Fujian, southeast China [*Xu et al*., 2013b], and the lack of measured precipitation data before 1951 may explain the reduced reliability of the GPCC data before 1951 in southeast China. The tree ring cellulose $\delta^{18}O$ series may be helpful to extend the precipitation records in this area. The reconstructed precipitation records correlated negatively ($r = -0.45$; 1870–2000) with DWI from four grid sites near the sampling site (Figure 8b), which indicates that the reconstructed precipitation reflects the regional hydroclimate. Although reconstructed May–October precipitation shows significant correlations with regional precipitation from GPCC v7 and DWI data, there are some differences between them. The reason that caused these differences may be that regional precipitation and DWI data reflect the climate at regional scale, while reconstructed May–October precipitation record detailed rainfall information at local scale.

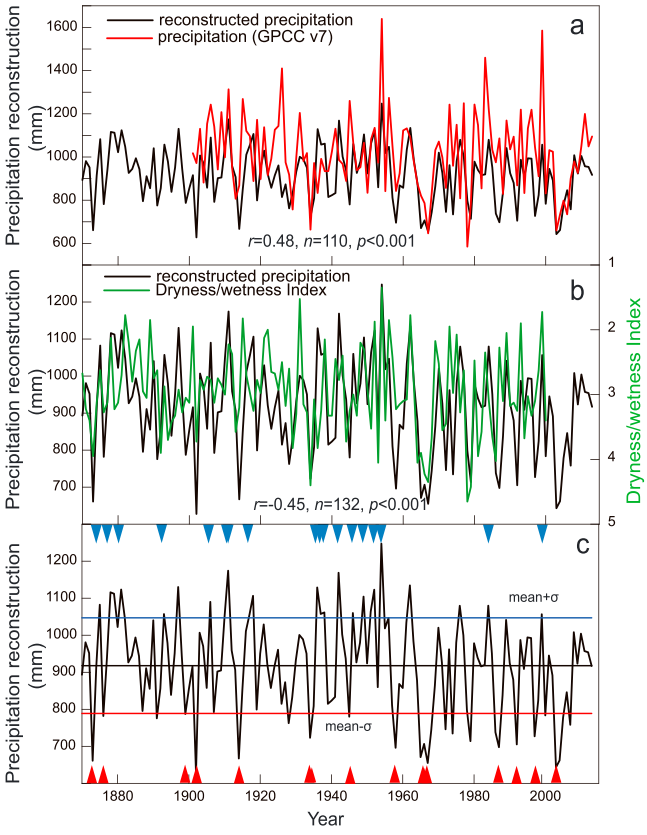

Figure 8. Comparison of the reconstructed precipitation (black line) and (a) precipitation data from GPCC v7, (b) the regional DWI, (c) local flood events (blue triangles), and drought events (red triangles) from documentary records.

Major local drought/flood events within 100 km of the sampling site (recorded in historical documents) are also shown by red/blue triangles in Figure 8c and Tables 4 and 5. For example, severe droughts in summer and autumn at Deqing and Gui'an caused a reduction in the grain yield in 1873 [*Wen*, 2006]. There was a severe drought in the summer of 1902 in Changhua, which is 35 km from the sampling site [*Wen*, 2006], and the reconstructed May–October precipitation was 628 mm (>2σ confidence level). There were flood events in May and August 1875 at Lin'an, which is about 20 km from the sampling site [*Wen*, 2006], and the reconstructed precipitation was 1082 mm (>1σ confidence level). Persistent rain at Changhua resulted in flash floods and huge economic losses in 1936 [*Wen*, 2006], and the reconstructed May–October precipitation was 1129 mm (>1σ confidence level). In total, approximately 76% of wet years identified by precipitation reconstruction were identified by documentary events [*Wen*, 2006]. Also, of 26 dry years identified by precipitation reconstruction, 58% were identified by documentary events [*Wen*, 2006]. The SEA was used to evaluate the relationship between extreme events from tree ring $\delta^{18}O$-based May–October precipitation reconstruction and extreme events from documentaries (Figure 9). The reconstructed May–October precipitation decreased/increased by around 200/170 mm when the extremely dry/wet events which were recorded in documentaries happened (Figures 9a and 9b). It also validates our precipitation reconstruction.

3.6. Relationship With ENSO

Spectral power analysis using the multitaper method [*Mann and Lees*, 1996] indicated that significant peaks in May–October reconstruction occurred at ~6.3, ~5, ~3.7, ~2.6, and ~2.3 years (Figure 10); all of the peaks fell within the range (2–7 years) of ENSO variability. Because ENSO-monsoon relationship was not stable [*Kumar et al*., 1999], we employed the 31 year running correlation analysis between them to explore the ENSO's influence on precipitation (Figure 11a). Negative correlations between reconstructed precipitation during the period of 1870–2013 existed, but it weakened during the period of 1920–1940 and before 1885. ENSO happened in tropics and affected climate in midlatitude areas by teleconnections. When variance of ENSO was high, ENSO teleconnection was strong [*J. Li et al*., 2011]. Because ENSO variance was relative low during the period of 1920–1960 [*Mason*, 2001; *Torrence and Webster*, 1999], which may result in weaken ENSO teleconnection in extratropical latitudes, other factors (e.g., SST in adjacent oceans and temperature in Tibetan Plateau) would exert the main influences on local climate. Figure 11c showed the significant positive correlation between precipitation reconstruction and SST in western Pacific during the period of 1920–1940. When summer SST in western Pacific is high, western Pacific subtropical high is strengthened, which results in more precipitation in the middle-lower valleys of Yangtze River [*Liu and Li*, 2011].

ENSO variance was relative high during the periods of 1875–1920 and 1961–2013 [*Torrence and Webster*, 1999], and SST in central tropical Pacific has significant influences on precipitation reconstruction

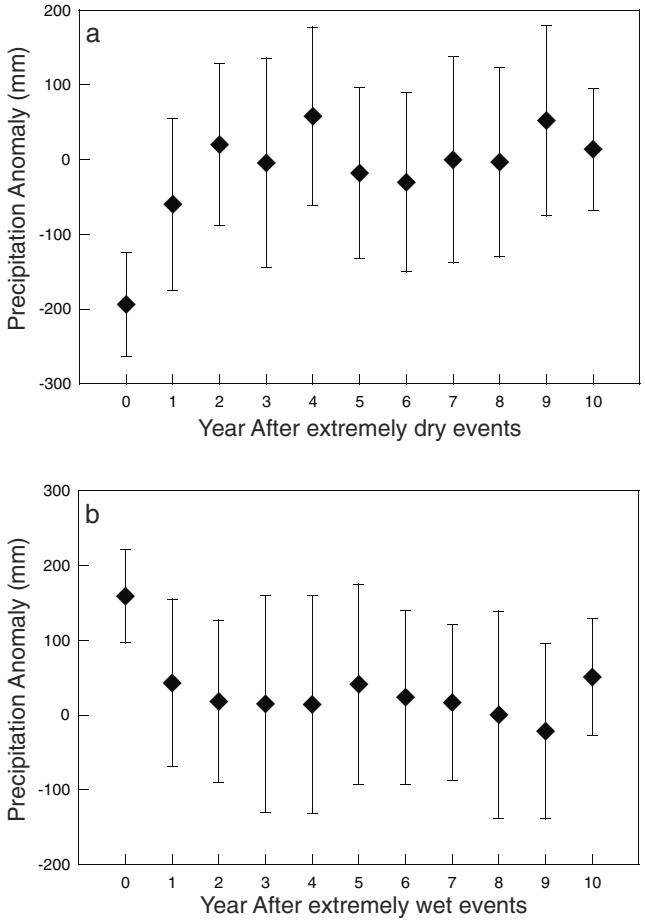

Figure 9. Reconstructed precipitation anomaly after extremely (a) dry and (b) wet years recorded in the documentaries; the bar indicates the one standard deviation.

(Figures 11b and 11d). ENSO can affect rainfall in the lower reaches of the Yangtze River by Indian summer monsoon (ISM) and East Asian summer monsoon (EASM), because water vapor in study area was supplied by ISM and EASM [*Zhou and Yu*, 2005; *Tang et al.*, 2015]. The analysis between precipitation in East China and ENSO showed that there was less summer rainfall over the middle and lower reaches of the Yangtze River when El Niño happened [*Kong and Tu*, 2003]. The unstable relationship between tree ring δ^{18}O-based

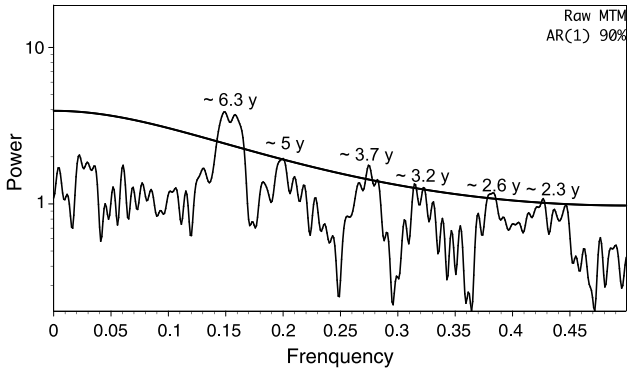

Figure 10. Multitaper method power spectra for the reconstructed precipitation from 1870 to 2013.

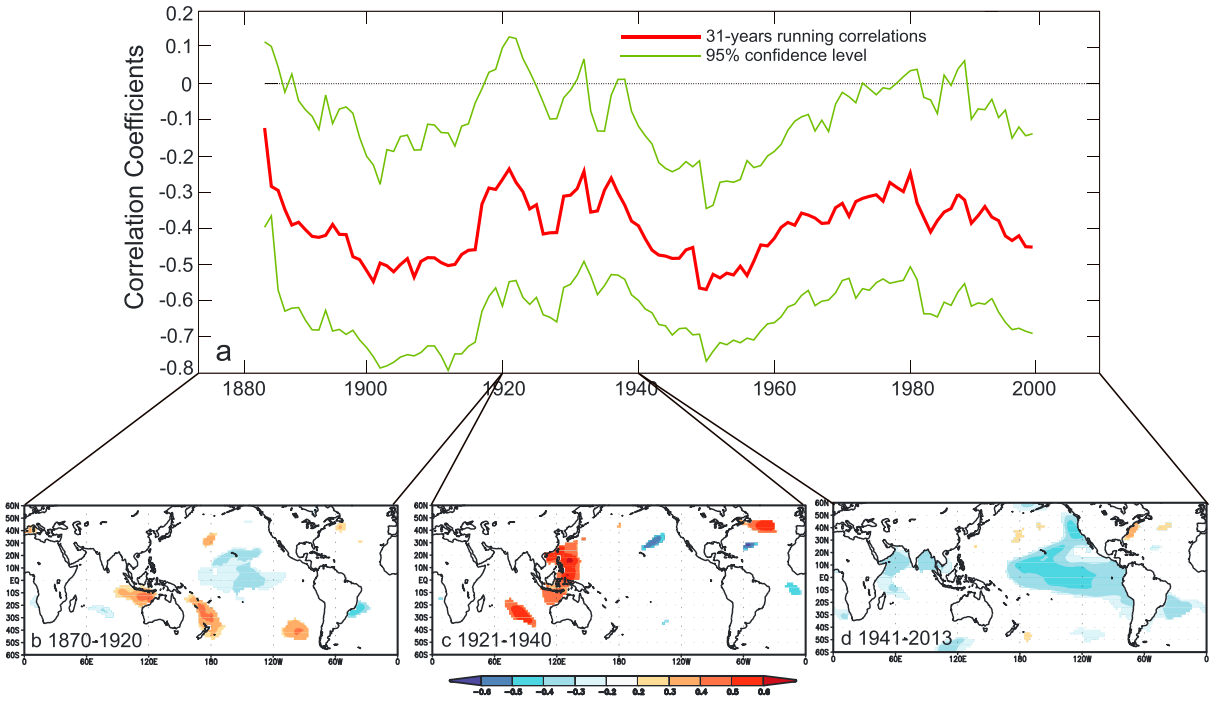

Figure 11. The 31 year running correlations between reconstructed May–October precipitation and May–October Niño3.4 index; (a) the confidence level was calculated by a Monte Carlo method. Spatial correlations between reconstructed May–October precipitation and May–October SST in the periods of (b) 1870–1920, (c) 1921–1940, and (d) 1941–2013.

monsoon season climate and ENSO was also found in southwest China [*Liu et al*., 2011], southeast China [*Xu et al*., 2013b], Himalaya [*Sano et al*., 2013], and Japan [*Sakashita et al*., 2015].

We investigated the relationship between ENSO and local extreme events in study area based on the extreme events derived from tree ring $\delta^{18}O$ and documentary and classified ENSO events from *Gergis and Fowler* [2009]. In Table 4, we can see that most of the extremely wet years of the study area followed La Niña events in the previous or current year. Several extremely wet events from 1936 to 1942 were not corresponding to La Niña events, because the correlations between SST in central tropical Pacific and precipitation weakened. There was a similar connection between extremely dry years and El Niño events (Table 5). Such correlation suggested that both El Niño and La Niña events strongly affect the local extreme events in the study area.

4. Conclusions

In this study, we investigated the interannual and intraannual variations in tree ring cellulose $\delta^{18}O$ in *P. taiwanensis* in the lower reaches of the Yangtze River in southeast China to explore its potential use in reconstructing precipitation. We found that the intraannual variations in tree ring cellulose $\delta^{18}O$ of *P. taiwanensis* show well-defined annual cycles, which generally followed seasonal patterns of precipitation $\delta^{18}O$. By comparing seasonal pattern of tree ring $\delta^{18}O$ in typhoon and nontyphoon years, seasonal patterns of tree ring $\delta^{18}O$ were influenced by August–October typhoons, which was helpful to identify typhoon in the past. Based on comparison between the $\delta^{18}O$ chronologies of young and old trees, we found that no juvenile effect on $\delta^{18}O$ was present for *P. taiwanensis* in the study area.

A correlation analysis between the tree ring $\delta^{18}O$ and precipitation indicated that the tree ring cellulose $\delta^{18}O$ is a suitable proxy for reconstructing May–October precipitation. The extreme events identified by tree ring $\delta^{18}O$-based reconstructed precipitation had been consistent with extreme events recorded from documentaries. Most of the extremely wet/dry events that were recorded by tree ring $\delta^{18}O$ and documentaries in the study area followed La Niña/El Niño events in the previous or current year. In addition, reconstructed precipitation showed significant relationship with central tropical Pacific SST. Both of which

indicated that ENSO had influences on May–October precipitation from the lower reaches of the Yangtze River. However, the relationship between ENSO and precipitation weakened between 1920 and 1940, and low variance of ENSO from 1920 to 1940 may be the reason that caused the reduced ENSO influences on precipitation in southeast China.

Acknowledgments

We are grateful to Shi who provided the meteorological data. The project was supported by Chinese Academy of Sciences Pioneer Hundred Talents Program a research grant from National Natural Science Foundation of China (41372362 and 31270659), National Basic Research Program of China (2015CB953803), and the Open Fund of Key Laboratory for Subtropical Mountain Ecology (Ministry of Science and Technology and Fujian Province funded); an environmental research grant from the Sumitomo Foundation, Japan; an FS research grant from Research Institute of Humanity and Nature, Kyoto, Japan; grant in-aid for Japan Society for the Promotion of Sciences Fellows (23242047 and 23-10262). The tree ring cellulose oxygen isotope data in this paper are available from the authors upon request (xuchenxi@gmail.com). We deeply appreciate the helpful comments from two anonymous reviewers and Louis Scuderi to improve the manuscript.

References

Araguas-Araguas, L., K. Froehlich, and K. Rozanski (1998), Stable isotope composition of precipitation over Southeast Asia, *J. Geophys. Res.*, *103*(D22), 28,721–28,742, doi:10.1029/98JD02582.

Cook, E. R., D. M. Meko, D. W. Stahle, and M. K. Cleaveland (1999), Drought reconstructions for the continental United States, *J. Clim.*, *12*(4), 1145–1162.

Dansgaard, W. (1964), Stable isotopes in precipitation, *Tellus*, *16*(4), 436–468.

Duan, J., Q. Zhang, L. Lv, and C. Zhang (2012), Regional-scale winter-spring temperature variability and chilling damage dynamics over the past two centuries in southeastern China, *Clim. Dyn.*, *39*, 919–928, doi:10.1007/s00382-011-1232-9.

Duan, J., Q. Zhang, and L. Lv (2013), Increased variability in cold-season temperature since the 1930s in subtropical China, *J. Clim.*, *26*, 4749–4757, doi:10.1175/JCLI-D-12-00332.1.

Esper, J., D. Frank, G. Battipaglia, U. Büntgen, C. Holert, K. Treydte, R. Siegwolf, and M. Saurer (2010), Low-frequency noise in $\delta^{13}C$ and $\delta^{18}O$ tree ring data: A case study of *Pinus uncinata* in the Spanish Pyrenees, *Global Biogeochem. Cycles*, *24*, GB4018, doi:10.1029/2010GB003772.

Evans, M., and D. Schrag (2004), A stable isotope-based approach to tropical dendroclimatology, *Geochim. Cosmochim. Acta*, *68*, 3295–3305.

Feng, X., H. Cui, K. Tang, and L. Conkey (1999), Tree-ring δD as an indicator of Asian monsoon intensity, *Quat. Res.*, *51*, 262–266.

Fritts, H. C. (1976), *Tree Rings and Climate*, Academic, London.

Fudeyasu, H., K. Ichiyanagi, A. Sugimoto, K. Yoshimura, A. Ueta, M. D. Yamanaka, and K. Ozawa, (2008), Isotope ratios of precipitation and water vapor observed in Typhoon Shanshan, *J. Geophys. Res.*, *113*(D12), doi:10.1029/2007JD009313.

Ge, Q., J. Zheng, Z. Hao, P. Zhang, and W. Wang (2005), Reconstruction of historical climate in China: High-resolution precipitation data from Qing dynasty archives, *Bull. Am. Meteorol. Soc.*, *86*(5), 671—679.

Gergis, J. L., and A. M. Fowler (2009), A history of ENSO events since AD 1525: Implications for future climate change, *Clim. Change*, *92*(3), 343–387.

Gessler, A., E. Brandes, N. Buchmann, G. Helle, H. Rennenberg, and R. Barnard (2009), Tracing carbon and oxygen isotope signals from newly assimilated sugars in the leaves to the tree ring archive, *Plant Cell Environ.*, *32*, 780–795.

He, Y., G. Fan, X. Zhang, D. Gao, and B. Hu (2012), Vegetation phenology monitoring and spatio-temporal dynamics in Zhejiang Province in past 10 years [in Chinese], *Chin. Agric. Sci. Bull.*, *28*(16), 117–124.

Holmes, R. (1983), Computer-assisted quality control in tree-ring dating and measurement, *Tree-Ring Bull.*, *43*(1), 69–78.

Huang, Y., H. Wang, K. Fan, and Y. Gao (2015), The western Pacific subtropical high after the 1970s: Westward or eastward shift?, *Clim. Dyn.*, 2035–2047.

Kanner, L. C., N. H. Buenning, L. D. Stott, and D. W. Stahle (2013), Climatologic and hydrologic influences on the oxygen isotope ratio of tree cellulose in coastal Southern California during the late 20th century, *Geochem. Geophys. Geosyst.*, *14*, 4488–4503, doi:10.1002/ggge.20256.

Kong, C., and Q. Tu (2003), Influence of El Niño events on summer precipitation in east China under different climatic backgrounds [in Chinese], *J. Nanjing Inst. Meteorol.*, *2003*(26), 84–88.

Kumar, K. K., B. Rajagopalan, and M. A. Cane (1999), On the weakening relationship between the Indian monsoon and ENSO, *Science*, *284*(5423), 2156–2159, doi:10.1126/science.284.5423.2156.

Labuhn, I., V. Daux, M. Pierre, M. Stievenard, O. Girardclos, A. Féron, D. Genty, V. Masson-Delmotte, and O. Mestre (2013), Tree age, site and climate controls on tree ring cellulose $\delta^{18}O$: A case study on oak trees from south-western France, *Dendrochronologia*, doi:10.1016/j.dendro.2013.11.001.

Li, J., S. Xie, E. Cook, G. Huang, R. D'Arrigo, F. Liu, J. Ma, and X. Zheng (2011), Interdecadal modulation of El Niño amplitude during the past millennium, *Nat. Clim. Change*, 114–118.

Li, Q., T. Nakatsuka, K. Kawamura, Y. Liu, and H. Song (2011), Regional hydroclimate and precipitation $d^{18}O$ revealed in tree-ring cellulose $\delta^{18}O$ from different tree species in semi-arid northern China, *Chem. Geol.*, *282*, 19–28, doi:10.1016/j.chemgeo.2011.01.004.

Liu, J. R., X. F. Song, G. F. Yuan, X. M. Sun, X. Liu, and S. Q. Wang (2010), Characteristics of $\delta^{18}O$ in precipitation over eastern monsoon China and the water vapor sources, *Chin. Sci. Bull.*, *55*(2), 200–211.

Liu, N., and Z. Li (2011), Relationship of the western Pacific warm pool SST anomaly and summer precipitation in China, *Meteorol. Disaster Reduct. Res.*, *34*(2), 8–13.

Liu, X., W. An, K. Treydte, X. Shao, S. Leavitt, S. Hou, T. Chen, W. Sun, and D. Qin (2011), Tree-ring $\delta^{18}O$ in southwestern China linked to variations in regional cloud cover and tropical sea surface temperature, *Chem. Geol.*, *291*, 104–115, doi:10.1016/j.chemgeo.2011.10.001.

Managave, S., M. Sheshshayee, H. Borgaonkar, and R. Ramesh (2010), Past break-monsoon conditions detectable by high resolution intra-annual $\delta^{18}O$ analysis of teak rings, *Geophys. Res. Lett.*, *37*, L05702, doi:10.1029/2009GL041172.

Mann, M., and J. Lees (1996), Robust estimation of background noise and signal detection in climatic time series, *Clim. Change*, *33*(3), 409–445.

Mason, S. J. (2001), El Niño, climate change, and southern African climate, *Environmetrics*, *12*(4), 327–345.

Meinzer, F., J. Brooks, J. Domec, B. Gartner, J. Warren, D. Woodruff, K. Bible, and D. Shaw (2006), Dynamics of water transport and storage in conifers studied with deuterium and heat tracing techniques, *Plant Cell Environ.*, *29*, 105–114.

Miller, D., C. Mora, H. Grissino-Mayer, C. Mock, M. Uhle, and Z. Sharp (2005), Tree-ring isotope records of tropical cyclone activity, *Proc. Natl. Acad. Sci. U.S.A.*, *103*, 14,294–14,297.

Qian, J., J. Lu, Q. Tu, and S. Wang (2002a), Reconstruction of the climate in the Tianmu Mountain area, Zhejiang Province, in the last 160 years by $\delta^{13}C$ sequence of tree ring α-cellulose, *Sci. China (Ser. D)*, *45*(5), 409–419.

Qian, J., Z. Deng, Q. Tu, S. Wang, and Y. Huang (2002b), Climatic significance of δD time series in tree rings from Tianmu Mountain, *Sci. China (Ser. D)*, *44*(12), 1140–1146.

Qian, W., Z. Yu, and Y. Zhu (2006), Spatial and temporal variability of precipitation in East China from 1880 to 1999, *Clim. Res.*, *32*(3), 209–218.

Roden, J. S., G. Lin, and J. R. Ehleringer (2000), A mechanistic model for interpretation of hydrogen and oxygen isotope ratios in tree-ring cellulose, *Geochim. Cosmochim. Acta*, *64*(1), 21–35, doi:10.1016/S0016-7037(99)00195-7.

Sakashita, W., Y. Yokoyama, H. Miyahara, Y. Yamaguchi, T. Aze, S. Obrohta, and T. Nakatsuka (2015), Relationship between early summer precipitation in Japan and the El Niño-Southern and Pacific Decadal Oscillations over the past 400 years, *Quat. Int.*, doi:10.1016/j.quaint.2015.05.054.

Sano, M., R. Ramesh, M. Sheshshayee, and R. Sukumar (2011), Increasing aridity over the past 223 years in the Nepal Himalaya inferred from a tree-ring δ^{18}O chronology, *Holocene*, *22*, 809–817.

Sano, M., C. Xu, and T. Nakatsuka (2012), A 300-year Vietnam hydroclimate and ENSO variability record reconstructed from tree ring δ^{18}O, *J. Geophys. Res.*, *117*, D12115, doi:10.1029/2012JD017749.

Sano, M., P. Tshering, J. Komori, K. Fujita, C. Xu, and T. Nakatsuka (2013), May–October precipitation in the Bhutan Himalaya since 1743 as reconstructed from tree ring cellulose δ^{18}O, *J. Geophys. Res. Atmos.*, *118*, 8399–8410, doi:10.1002/jgrd.50664.

Shi, J. F., E. Cook, H. Lu, J. Li, W. Wright, and S. Li (2010), Tree-ring based winter temperature reconstruction for the lower reaches of the Yangtze River in southeast China, *Clim. Res.*, *41*, 169–175.

Smith, T. M., R. W. Reynolds, T. C. Peterson, and J. Lawrimore (2008), Improvements to NOAA's historical merged land-ocean surface temperature analysis (1880–2006), *J. Clim.*, *21*(10), 2283–2296, doi:10.1175/2007JCLI2100.1.

Song, J. (2000), Changes in dryness/wetness in China during the last 529 years, *Int. J. Climatol.*, *20*(9), 1003–1016.

Sperber, K. R., H. Annamalai, I.-S. Kang, A. Kitoh, A. Moise, A. Turner, B. Wang, and T. Zhou (2012), The Asian summer monsoon: An intercomparison of CMIP5 vs. CMIP3 simulations of the late 20th century, *Clim. Dyn.*, *41*(9–10), 2711–2744, doi:10.1007/s00382-012-1607-6.

Tang, Y., H. Pang, W. Zhang, Y. Li, S. Wu, and S. Hou (2015), Effects of changes in moisture source and the upstream rainout on stable isotopes in precipitation—A case study in Nanjing, eastern China, *Hydrol. Earth Syst. Sci.*, *19*, 4293–4306.

Torrence, C., and P. J. Webster (1999), Interdecadal changes in the ENSO-monsoon system, *J. Clim.*, *12*(8), 2679–2690, doi:10.1175/1520-0442(1999)012<2679:ICITEM>2.0.CO;2.

Vuille, M., R. Bradley, M. Werner, R. Healy, and F. Keimig (2003), Modeling δ^{18}O in precipitation over the tropical Americas: 1.Interannual variability and climatic controls, *J. Geophys. Res.*, *108*(D6), 4174, doi:10.1029/2001JD002038.

Vuille, M., M. Werner, R. Bradley, and F. Keimig (2005), Stable isotopes in precipitation in the Asian monsoon region, *J. Geophys. Res.*, *110*, D23108, doi:10.1029/2005JD006022.

Wen, K. (2006), *Meteorological Disasters in China*, China Meteorological Press, Beijing, China.

Wigley, T., K. Briffa, and P. Jones (1984), On the average value of correlated time series, with applications in dendroclimatology and hydrometeorology, *J. Climate Appl. Meteorol.*, *23*(2), 201–213, doi:10.1175/1520-0450(1984)023<0201:OTAVOC>2.0.CO;2.

Wu, G., Z. Hao, and J. Zheng (2010), Reconstruction and analysis of seasonal precipitation in Nanjing since 1736 [in Chinese], *Sci. Geogr. Sin.*, *6*, 936–942.

Xie, L., G. Wei, W. Deng, and X. Zhao (2011), Daily δ^{18}O and δD of precipitations from 2007 to 2009 in Guangzhou, south China: Implications for changes of moisture sources, *J. Hydrol.*, *400*(3-4), 477–489, doi:10.1016/j.jhydrol.2011.02.002.

Xu, C., M. Sano, and T. Nakatsuka (2011), Tree ring cellulose δ^{18}O of *Fokienia hodginsii* in northern Laos: A promising proxy to reconstruct ENSO?, *J. Geophys. Res.*, *116*, D24109, doi:10.1029/2011JD016694.

Xu, C., M. Sano, and T. Nakatsuka (2013a), A 400-year record of hydroclimate variability and local ENSO history in northern Southeast Asia inferred from tree-ring δ^{18}O, *Palaeogeogr. Palaeoclimatol. Palaeoecol.*, *386*, 588–598.

Xu, C., H. Zheng, T. Nakatsuka, and M. Sano (2013b), Oxygen isotope signatures preserved in tree ring cellulose as a proxy for April–September precipitation in Fujian, the subtropical region of southeast China, *J. Geophys. Res. Atmos.*, *118*, 12,805–12,815, doi:10.1002/2013JD019803.

Xu, C., M. Sano, K. Yoshimura, and T. Nakatsuka (2014), Oxygen isotopes as a valuable tool for measuring annual growth in tropical trees that lack distinct annual rings, *Geochem. J.*, *48*, 371–378.

Xu, C., N. Pumijumnong, T. Nakatsuka, M. Sano, and Z. Li (2015), A tree-ring cellulose δ^{18}O-based July-October precipitation reconstruction since AD 1828, northwest Thailand, *J. Hydrol.*, doi:10.1016/j.jhydrol.2015.02.037.

Xu, C., H. Zheng, T. Nakatsuka, M. Sano, and Z. Li (2016), Inter- and intra-annual tree-ring cellulose oxygen isotope variability in response to precipitation in southeast China, *Trees: Struct. Funct.*, doi:10.1007/s00468-015-1320-2.

Xu, H., Y. Hong, and B. Hong (2012), Decreasing Asian summer monsoon intensity after 1860 AD in the global warming epoch, *Clim. Dyn.*, *39*, 2079–2088.

Yang, F., F. Shi, S. Kang, S. Wang, Z. Xiao, T. Nakatsuka, and J. Shi (2013), Comparison of the dryness/wetness index in China with the Monsoon Asia Drought Atlas, *Theor. Appl. Climatol.*, doi:10.1007/s00704-013-0858-4.

Yen, C. (1972), Study on the root system form and distribution habit of the ligneous plants for soil conservation in Taiwan (preliminary report), *J. Chin. Soil Water Conserv.*, *3*, 179–204.

Yoshimura, K., M. Kanamitsu, D. Noone, and T. Oki (2008), Historical isotope simulation using reanalysis atmospheric data, *J. Geophys. Res.*, *113*, D19108, doi:10.1029/2008JD010074.

Zhang, D. (1988), The method for reconstruction of the dryness/wetness series in China for the last 500 years and its reliability [in Chinese], in *The Reconstruction of Climate in China for Historical Times*, pp. 18–30, Science Press, Beijing.

Zhang, D., Y. Liu, Y. Liang, and J. Li (2005), Reconstruction of annual and seasonal precipitation series of Nanjing, Suzhou and Hangzhou during the 18th century [in Chinese], *Quat. Sci.*, *25*(2), 121–129.

Zhao, X., J. Wang, J. Qian, and X. Jiang (2005), The climate change in autumn recorded in the δ^{13}C of tree rings in the past 300 years at Tianmu Mountain [in Chinese], *J. Mt. Res.*, *23*(5), 540–549.

Zhou, T., B. Wu, and B. Wang (2009), How well do atmospheric general circulation models capture the leading modes of interannual variability of Asian-Australian monsoon?, *J. Clim.*, *22*, 2199–2215.

Zhou, T. J., and R. Yu (2005), Atmospheric water vapor transport associated with typical anomalous summer rainfall patterns in China, *J. Geophys. Res.*, *110*, D08104, doi:10.1029/2004JD005413.